3) Therefore, the best-match aerodynamic influence matrix which ensures that experimental data be exactly fit is such that

$$\begin{cases} \Delta c_{p1} = 2.55442\alpha_1 + 0.55599\alpha_2 + 0.17172\alpha_3 + 0.06187\alpha_4 \\ \Delta c_{p2} = 0.99171\alpha_1 + 2.24172\alpha_2 + 0.40397\alpha_3 + 0.11320\alpha_4 \\ \Delta c_{p3} = 0.54344\alpha_1 + 0.71843\alpha_2 + 1.18315\alpha_3 + 0.34038\alpha_4 \\ \Delta c_{p4} = 0.30923\alpha_1 + 0.35451\alpha_2 + 0.60457\alpha_3 + 0.60509\alpha_4 \end{cases} \quad (7)$$

Concluding Remarks

A procedure has been developed which finds minimum changes in an analytical aerodynamic influence matrix to make it exactly agree with a set of measured pressure coefficients. It is suitable for application to large matrices where the number of linearly independent sets of available pressure coefficient data is smaller than the total number of panels of the aerodynamic discretization. Provisions for overcoming a nonsimilarity between the experimental and the theoretical aerodynamic grid, as well as aeroelastic effects on the experimental model are straightforward.

References

[1]Fornasier, L., and D'Espiney, P., "Prediction of Stability Derivatives for Missiles Using the HISSS Panel Code," AGARD-CP 451, March 1989.

[2]Woodward, F. A., "An Improved Method for the Aerodynamic Analysis of Wing-Body-Tail Configurations in Subsonic and Supersonic Flow," NASA CR-2228, 1973.

[3]Bertin, J. J., and Smith, M. L., "*Aerodynamics for Engineers*," Prentice Hall, Englewood Cliffs, NJ, 1979, pp. 187–207.

[4]Berman, A., and Nagy, E. J., "Improvement of a Large Analytical Model Using Test Data," *AIAA Journal*, Vol. 21, No. 8, 1983, pp. 1168–1173.

[5]"FASTOP: An Automated Procedure for Flutter and Strength Analysis and Optimization of Aerospace Vehicles," Program User's Manual, Vol. II, Air Force Flight Dynamics Lab., Wright-Patterson AFB, OH, Dec. 1975, pp. 62–72.

Computational Flowfields for Static Testing of Powered Hypersonic Aftbody Models

Lawrence D. Huebner*
NASA Langley Research Center, Hampton, Virginia 23665

Introduction

HYPERSONIC air-breathing vehicles, such as the national aero-space plane (NASP), utilize a supersonic combustion ramjet (scramjet) propulsion system. The location of this scramjet on the underside of the airframe, and the shaping of the forebody and aftbody are prime concerns of propulsion/airframe integration (PAI) to provide optimum aero-propulsive performance. The forebody acts as a precompression region for the inlet flow where the objective is to obtain a high-quality compressed flow to the scramjet inlet while maintaining low-forebody drag. The aftbody, in part, serves as the external scramjet nozzle expansion for the exhaust gases and provides significant force and moment components for the entire vehicle. Consequently, efficient PAI is very important in the design of hypersonic, airbreathing vehicles like the NASP.[1]

PAI is an important facet in the aerodynamic analysis and testing of such NASP-like hypersonic, air-breathing vehicles under simulated powered conditions. Ground-based testing of powered hypersonic, air-breathing configurations is both difficult and expensive due to the high temperatures and pressures necessary to sustain the hydrogen/air combustion proess.[2] Also, size limitations of ground-based facilities preclude duplication of scramjet operation because the combustion process is not geometrically scalable.[2] Furthermore, numerical modeling of the combustion process is expensive, being feasible only with the most powerful supercomputers. In order to obtain powered data and avoid these problems, an experimental technique was developed to simulate the hydrogen/air scramjet exhaust, whereby the inlet is faired over and a simulant gas is routed into a plenum in the model. The simulant gas passes through a combustor nozzle designed for inviscid similitude of the actual combustion process at the combustor exit, and then expands into the aftbody flowfield. The models employing this technique can either be fully metric, utilizing a flow-through balance, have metric and nonmetric parts, or be highly instrumented for surface pressure integration. In either of the last two techniques, it is possible to isolate the aftbody nozzle during powered testing to determine the component force and moment contributions.

To date, powered tests have been performed in hypersonic wind tunnels to provide some freestream similitude with typical flight conditions. However, it is uncertain if the hypersonic (dynamic) environment is truly required for testing powered aftbodies. It has been shown that, at typical values of static nozzle pressure ratio (SNPR, the ratio of the static pressure at the combustor exit to the freestream static pressure), differences in aftbody pressure distributions are insignificant as the freestream Mach number is increased from 4.0 to 14.0 at constant Reynolds number.[3] This then leads to the possibility of an alternate form of powered testing. If an appropriate simulation parameter (like SNPR) can be matched by reducing the pressure of the test section to the local freestream pressure that occurs in the hypersonic flowfield, powered aftbody testing in a static environment may be possible. This technique would allow the model to be much simpler (no realistic forebody required) with a significant decrease in the fabrication and testing expenses. This note presents the method and results of a two-dimensional computational study aimed at assessing the feasibility of conducting static tests to determine the performance of hypersonic, air-breathing aftbody models.

Computational Method

The computational fluid dynamics (CFD) code applied to the configurations of interest in this study is the general aerodynamic simulation program (GASP).[4,5] GASP solves the integral form of the governing equations, including the full Reynolds-averaged Navier-Stokes equations, the thin-layer Navier-Stokes (TLNS) equations, the parabolized Navier-Stokes (PNS) equations, and the Euler equations. The discretized equations may be solved by space-marching or global-iteration, and both explicit multistage Runge-Kutta and implicit time integration schemes are included. The code allows highly flexible coupling of multiple grid zones, each of which may be solved independently or simultaneously. Grid generation for GASP is simplified due to the zonal algorithm, but grid point connectivity is required along the zonal interface boundaries. The

Presented as Paper 91-1709 at the AIAA 22nd Fluid Dynamics, Plasma Dynamics, and Lasers Conference, Honolulu, HI, June 24–26, 1991; received Nov. 30, 1991; revision received Jan. 9, 1992; accepted for publication Jan. 9, 1992.

*Aerospace Engineer, Hypersonics Group Leader, Supersonic/Aerodynamics Branch, Applied Aerodynamics Division, M/S 413. Senior Member AIAA.

inputs are defined in two types of files: 1) one specifying zonal interactions; and 2) the other controlling the solution within an individual zone. The solution algorithms, flux models and limiters, viscous models, boundary conditions, and initial flow conditions, are all set for each zone within the input files. Necessary data for restarting and/or postprocessing is saved in two output files.

Before GASP (or any CFD code) can be used as an analysis tool, code calibration is essential for the types of flows of interest, providing a level of confidence in the ability of the code to accurately predict the fluid dynamics of the problem. Previous studies have shown that GASP is capable of simulating the aftbody flows associated with powered hypersonic, air-breathing vehicles, lending credibility to GASP for this class of problem.[3,6] Reference 3 provides a qualitative comparison of powered-aftbody schlieren photographs with GASP solutions. Reference 6 provides a quantitative comparison of GASP solutions with experimental data consisting of powered-aftbody surface and flowfield pressures. References 3 and 6 show that viscous analysis is required for accurate determination of powered aftbody forces and moments, as well as powered aftbody flowfield features.

Computational Procedure

Computationally, the external flow was initialized with constant freestream conditions at the nose and proceeds past the powered hypersonic vehicle lower-surface centerline geometry, while the internal flow begins at the throat of the scramjet nozzle where the flow is sonic and assumed to have constant conditions spanning the nozzle height (i.e., no preset boundary layer). A three-zone grid was used to perform the CFD analysis. The first zone was for the forebody from the nose to the cowl trailing edge. The second zone consisted of the internal part of the nozzle, and the third zone modeled the aftbody into which the two upstream zonal solutions propagated. The total number of points in this two-dimensional grid was about 67,000. The grid points were clustered near the body to provide accurate resolution of the boundary layer for viscous calculations. The inner-law variable y^+ provides a measure of accuracy of the viscous solutions by combining density, velocity, and viscosity with the amount of normal point-spacing at the first computational cell center off the body. Typically y^+ values on the order of one will provide adequate viscous resolution.[7] For this effort, values were less than two, except in the region where the boundary layer was beginning to develop (near the nose and just downstream of the nozzle throat). Convergence and numerical accuracy issues related to this study are similar to those presented in Ref. 3 and will not be addressed here.

For this study, the freestream external flow and the internal exhaust gas are assumed to be air, modeled as a perfect gas. The internal (jet) conditions are initialized at the nozzle throat with $M_{\text{jet}} = 1.0$, $p_{t,\text{jet}} = 30$ psia, and $T_{t,\text{jet}} = 100°\text{F}$. These conditions yield an average static pressure at the combustor exit of 4.867 psia. Normalizing this by the freestream pressure for a specific case produces the value of SNPR.

Since, GASP solutions cannot be obtained for a $M_\infty = 0.0$ flow, a solution was initiated at a very low Mach number, referred to herein as "pseudostatic." This pseudostatic solution ($M_\infty = 0.10$) was compared with a PNS solution at $M_\infty = 6.0$ and $Re_\infty = 2.0 \times 10^6$/ft. The freestream pressure for both solutions was 0.063 psia, which yielded the same SNPR of 77. Furthermore, the pseudostatic case is a mixed subsonic/supersonic problem, so the TLNS equations must be solved. The solution converged to slightly over three orders of magnitude in residual reduction in 2000 global iterations. The solution did not converge further because GASP is a compressible code where the residual is based in part on density values which, in this case, are extremely small and invariant in the external flow. An incompressible code would be better for the external flow computationally, but compressibility is required for the powered aftbody flow. The aftbody surface pressure convergence history showed that steady state appeared to have been achieved at 2000 iterations since they did not vary by more than 0.3% of the aftbody pressure values obtained at three-orders-of-magnitude reduction.

Results

A comparison of the flowfields (shown by Mach number contours) for the hypersonic and pseudostatic solutions (Fig. 1) indicates that the plume for the pseudostatic case expands farther into the freestream than for the hypersonic case. This may have important consequences in extending this analysis to three dimensions, since the aftbody, wings, and control surfaces may or may not be completely inside the static nozzle flow compared to a dynamic case at similar SNPR. A comparison of aftbody surface pressure values (from the cowl trailing-edge location to the end of the vehicle) for these two solutions is shown in Fig. 2 and are quite similar with some small differences near the beginning of the aftbody. A comparison of the aftbody lift, thrust (both in pounds per unit span), and pitching moment (in inch-pounds per unit span) values are obtained by integrating the differential pressures $(p - p_\infty)$ on the aftbody and using a moment center located at the expansion corner of the combustor exit. It can be seen that the integrated pressures for the first two cases agree with each other to within 4%.

However, the question arises as to whether a parameter other than SNPR should be used as a comparative factor between static- and dynamic-powered testing. Figure 1 shows that the plume for the hypersonic case is not directly influenced by the freestream pressure due to the series of compression and expansion disturbances caused by the local flow conditions in the external flow near the cowl trailing edge. With this is mind, a new reference pressure was chosen for the pseudostatic case by examining the flowfield static pressure

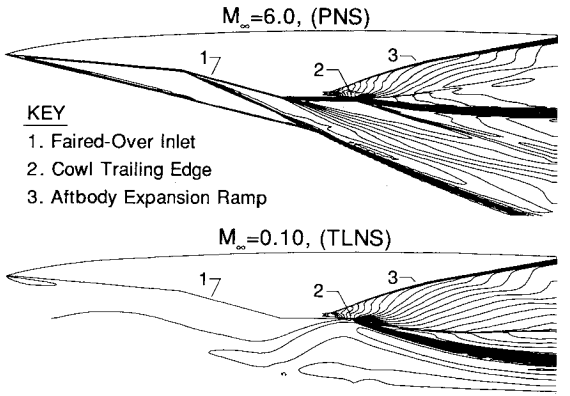

Fig. 1 Flowfield comparison of pseudostatic- and dynamic-powered simulation for the powered hypersonic vehicle model with constant SNPR = 77, Mach number contours.

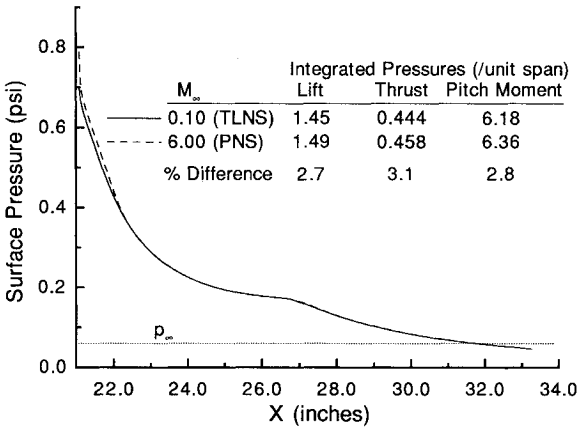

Fig. 2 Afterbody surface pressure comparison of pseudostatic- and dynamic-powered simulation for the powered hypersonic vehicle model with constant SNPR = 77.

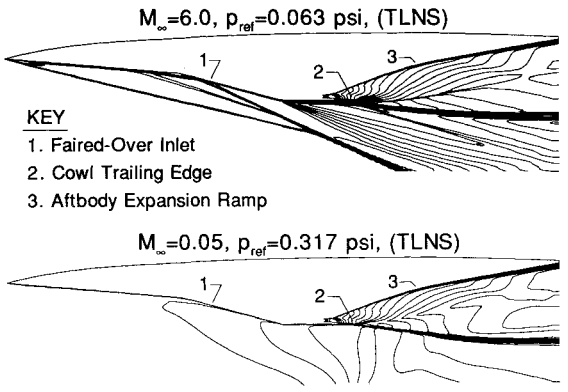

Fig. 3 Flowfield comparison of pseudostatic- and dynamic-powered simulation for the powered hypersonic vehicle model with consistent reference pressure near the plume, Mach number contours.

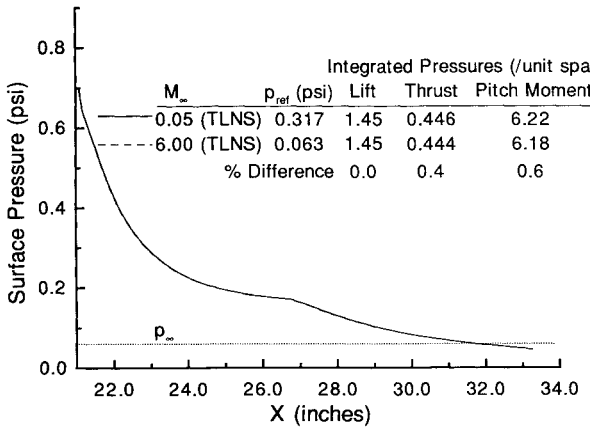

Fig. 4 Afterbody surface pressure comparison of pseudostatic- and dynamic-powered simulation for the powered hypersonic vehicle model with consistent reference pressure near the plume.

in the local flow region between the external cowl-trailing-edge shock and the plume near the cowl trailing edge. The value for this reference static pressure was five times the freestream static pressure, or 0.317 psia. A new pseudostatic TLNS solution was computed, this time at $M_\infty = 0.05$, which was possible because the solution became more stable using the higher reference pressure.

In addition to the question of appropriate choice of reference pressure, the difference in the aftbody surface pressures near the cowl trailing edge (Fig. 2) may have been due to the numerical modeling instead of the physical conditions, since one result was a PNS solution and the other was a TLNS solution. Therefore, a new hypersonic solution was also computed at the same conditions as before, namely, $M_\infty = 6.0$ and $Re_\infty = 2.0 \times 10^6$/ft, and $p_\infty = 0.063$ psia, but using the TLNS equations instead of the PNS equations.

The new solutions converged with a reduction in the global residual of four orders of magnitude in 868 and 1201 iterations for the pseudostatic and hypersonic cases, respectively. A comparison of flowfields shown in Fig. 3 reveals that the plume location for the pseudostatic solution is very close to that for the hypersonic case. The location of the plume in the hypersonic solution did not change by applying the TLNS equations to the problem. Examination of the aftbody surface pressures for the two TLNS solutions (Fig. 4) shows nearly identical pressure distributions and integrated force and moment components. Furthermore, the force and moment components from the pseudostatic solution shown in Fig. 2 are also nearly identical to those from the pseudostatic solution shown in Fig. 4, implying that the 3% difference seen in Fig. 2 is not caused by the use of a different reference pressure, but is actually a numerical phenomenon associated with the equation set being solved.

Conclusions

Two-dimensional CFD analyses have been presented related to the ground testing of hypersonic, air-breathing models that feature scramjet exhaust flow simulation. CFD analysis shows that it is possible to test aftbody powered hypersonic airbreather configurations in a static, pumped-down environment to obtain aftbody aerodynamic performance data. However, the analysis shows that a tunnel static pressure must be used in order to provide a comparable reference pressure that occurs at the location where the plume propagates off the cowl trailing edge in the hypersonic flow, instead of simply using the freestream static pressure that would be achieved in the hypersonic flowfield.

References

[1]Edwards, C. L. W., Small, W. J., Weidner, J. P., and Johnston, P. J., "Studies of Scramjet/Airframe Integration Techniques for Hypersonic Aircraft," AIAA Paper 75-58, Pasadena, CA, Jan. 1975.

[2]Hartill, W. R., "Method for Obtaining Aerodynamic Data on Hypersonic Configurations with Scramjet Exhaust Flow Simulation," NASA CR-2831, June 1977.

[3]Huebner, L. D., and Tatum, K. E., "Computational and Experimental Aftbody Flowfields for Hypersonic, Airbreathing Configurations with Scramjet Exhaust Flow Simulation," AIAA Paper 91-1709, Honolulu, HI, June 1991.

[4]Walters, R. W., Cinnella, P., Slack, D. C., and Halt, D., "Characteristic-Based Algorithms for Flows in Thermo-Chemical Nonequilibrium," AIAA Paper 90-0393, Reno, NV, Jan. 1990.

[5]Walters, R. W., Slack, D. C., Cinnella, P., Applebaum, M., and Frost, C., "A User's Guide to GASP, Revision 0," Virginia Polytechnic Inst. and State Univ., Blacksburg, VA, Nov. 1990.

[6]Tatum, K. E., Monta, W. J., Witte, D. W., and Walters, R. W., "Analysis of Generic Scramjet External Nozzle Flowfields Employing Simulant Gases," AIAA Paper 90-5242, Orlando, FL, Oct. 1990.

[7]Richardson, P. F., and Parlette, E. B., "Comparison Between Experimental and Numerical Results for a Research Hypersonic Aircraft," *Journal of Aircraft*, Vol. 27, No. 4, 1990, pp. 300-305.

Formulation of Design Envelope Criterion in Terms of Deterministic Spectral Procedure

J. G. Jones*
Defence Research Agency, RAE Farnborough, Hampshire, GU14 6TD, England, United Kingdom

Introduction

MANDATORY aircraft limit-load requirements for flight in continuous turbulence are generally met by using power-spectral procedures to compute the loads. Two methods are in general use: 1) design envelope approach, and 2) mission analysis. In the design envelope approach, a response factor $\bar{A}$ is calculated [Eq. (8)] and multiplied by a specified gust intensity U_σ to obtain the design load for a series of points throughout the design envelope. In mission analysis, mission profiles are analyzed in order to obtain probabilities of exceeding various load levels and a design probability is specified from which design loads may be found.

In this note we consider the design envelope approach and demonstrate that it can be reformulated in a manner which makes no distinction between linear and nonlinear response,

Received May 4, 1991; revision received Jan. 12, 1992; accepted for publication Jan. 20, 1992.

*Senior Principal Scientific Officer. Member AIAA.